One-Electron Transformations of Paramagnetic Cobalt Complexes. Synthesis and Structure of Cobalt(II) Amidodiphosphine Halide and Alkyl Complexes and Their Reaction with Alkyl Halides

Michael D. Fryzuk,* Daniel B. Leznoff, Robert C. Thompson, and Steven J. Rettig‡

Contribution from the Department of Chemistry, University of British Columbia, 2036 Main Mall, Vancouver, B.C., Canada V6T 1Z1

Received June 30, 1997

Abstract: Complexes of the type $CoX[N(SiMe_2CH_2PPh_2)_2]$, where X = Cl, Br, or I, can be prepared via reaction of CoX_2 with $LiN(SiMe_2CH_2PPh_2)_2$; these derivatives are tetrahedral high-spin d^7 systems. Reaction of these halide complexes with organolithium, sodium, or potassium reagents generates square-planar, low-spin hydrocarbyl complexes of the formula $CoR[N(SiMe_2CH_2PPh_2)_2]$ (R = Me, CH_2Ph, CH_2SiMe_3, C_5H_5). One-electron oxidations have been carried out; only the product of halide abstraction is observed. For example, addition of $PhCH_2X$ to the halide derivatives $CoX[N(SiMe_2CH_2PPh_2)_2]$ generates trivalent, paramagnetic complexes, $CoX_2[N(SiMe_2CH_2PPh_2)_2]$; these derivatives show variable-temperature magnetic susceptibility data that are consistent with zero-field splitting of the S = 1 state. Addition of methyl bromide or methyl iodide to low-spin $CoMe[N(SiMe_2CH_2PPh_2)_2]$ results in the formation of the Co(II) halide derivatives $CoX[N(SiMe_2CH_2PPh_2)_2]$ along with methane and bibenzyl. It is proposed that the Co(III) methyl halide complex $CoMe(X)[N(SiMe_2CH_2PPh_2)_2]$ is unstable and loses methyl radical homolytically to generate the Co(II) halide derivative; the methyl subsequently reacts with the toluene solvent to produce methane and bibenzyl. Addition of excess benzyl halides has also been found to generate the Co(II) halide complexes initially, followed by a one-electron oxidation to the Co(III) dihalide derivatives. In much of the one-electron chemistry of the Co(II) derivatives incorporating the amidodiphosphine ligand, the decomposition of the putative but unstable Co(III) alkyl halide derivative $CoRX[N(SiMe_2CH_2PPh_2)_2]$ is proposed as a recurring event.

Introduction

Electron transfer and radical processes figure prominently in many different areas of chemistry.[1−5] In organic chemistry, convenient and versatile sources of alkyl radicals are in demand to initiate a wide variety of reactions.[6,7] Polymerization with free radicals is arguably one of the most important industrial processes for high molecular weight polymers.[6] In transition metal chemistry, the discovery that the active site of vitamin B_{12} contains a readily homolyzable Co(III)−carbon bond[8,9] has fueled research into the preparation and reactivity of cobalt complexes,[10−16] particularly those species that can mimic coenzyme bioinorganic functions. That paramagnetic transition metal complexes provide a unifying theme to all of the above areas is not accidental; metal complexes with unpaired electrons are part of the fabric of coordination chemistry and are now becoming more prevalent in organometallic chemistry.

The reaction of alkyl halides with paramagnetic metal complexes has been the focus of numerous studies. Not only do these processes have relevance to radical-based organic transformations but they are probably one of the most common methods for the synthesis of vitamin B_{12} models, although other reagent types, including direct addition of in situ generated radicals to Co(II) systems,[17] have been described. Although most free radical polymerizations do not involve metal complexes, there is the recent discovery that living radical polymerizations can be achieved in the presence of Cu(II) derivatives. With regard to cobalt complexes, both one- and two-electron processes involving alkyl halides have been reported;[18−20] for example, the two-electron oxidative addition of alkyl halides to Co(I) derivatives (eq 1) is a classic route to Co(III) species:[21,22] Of particular significance is the addition of alkyl halides

‡ Professional Officer: UBC X-ray Structural Laboratory.

(1) Fossey, J.; Lefort, D.; Sorba, J. *Free Radicals in Organic Chemistry*; John Wiley & Sons: New York, 1995.
(2) Eberson, L. *Electron-Transfer Reactions in Organic Chemistry*; Springer-Verlag: Berlin, 1987.
(3) *Electron Transfer in Inorganic, Organic, and Biological Systems*; Bolton, J. R., Mataga, N., McLendon, G. L., Eds.; American Chemical Society: Washington, DC, 1991; Vol. 228.
(4) *Organometallic Radical Processes*; Trogler, W. C., Ed.; Elsevier: New York, 1990.
(5) *Macromol. Symp.* **1987**, *10−11*.
(6) Matyjaszewski, K.; Patten, T. E.; Xia, J. *J. Am. Chem. Soc.* **1997**, *119*, 674.
(7) Curran, D. P. *Synthesis* **1988**, 417.
(8) *B12*; Dolphin, D., Ed.; John Wiley & Sons: New York, 1982; Vols. 1 and 2.
(9) Toscano, P. J.; Marzilli, L. G. *Prog. Inorg. Chem.* **1984**, *31*, 105.
(10) Pattenden, G. *Chem. Soc. Rev.* **1988**, *17*, 361.
(11) Johnson, M. D. *Acc. Chem. Res.* **1983**, *16*, 343.
(12) Scheffold, R.; Rytz, G.; Walder, L. In *Modern Synthetic Methods*; Scheffold, R., Ed.; Wiley: Chichester, 1983; Vol. 3; p 355.
(13) Brown, T. M.; Cooksey, C. J.; Crich, D.; Dronsfield, A. T.; Ellis, R. *J. Chem. Soc., Perkin Trans.1* **1993**, 2131.
(14) Patel, V. F.; Pattenden, G.; Thompson, D. M. *J. Chem. Soc., Perkin Trans.1* **1990**, 2729.
(15) Branchaud, B. P.; Choi, Y. L. *J. Org. Chem.* **1988**, *53*, 4638.
(16) Baldwin, J. E.; Li, C.-S. *J. Chem. Soc., Chem. Commun.* **1987**, 166.
(17) Gridnev, A. A.; Ittel, S. D.; Fryd, M.; Wayland, B. B. *Organometallics* **1993**, *12*, 4871.
(18) Zhou, D.-L.; Walder, P.; Scheffold, R.; Walder, L. *Helv. Chim. Acta* **1992**, *75*, 995.
(19) Witman, M. W.; Weber, J. H. *Inorg. Chim. Acta* **1977**, *23*, 263.
(20) Dodd, D.; Johnson, M. D. *J. Organomet. Chem.* **1973**, *52*, 1.
(21) Coleman, W. M.; Taylor, L. T. *J. Am. Chem. Soc.* **1971**, *93*, 5446.

S0002-7863(97)02163-X CCC: $15.00
Published on Web 09/17/1998

$$L_nCo(I) + RX \longrightarrow L_nCo(III)RX \quad (1)$$

to Co(II) complexes to give Co(III) halide and Co(III) alkyl complexes in a series of two, one-electron redox, radical-based bimolecular reactions;[23] as indicated in Scheme 1, the stoichiometry involves 1 equiv of the Co(II) starting material reacting with 0.5 equiv of the alkyl halide.

Generally, the Co(II) systems studied have been low-spin, rigidly square planar systems (porphyrins, salen-type ligands) as these compounds are considered suitable models for the corrin framework in Vitamin B_{12},[24,25] although the addition of RX to $Co(CN)_5^{3-}$ shows that this reaction can be generalized beyond traditional planar tetradentate ligand-type complexes.[26−28] Despite this last example, however, studies involving alkyl halide addition reactions to *non*-chelating or *non*-macrocyclic Co(II) systems are not common. In one case, addition of alkyl halides to cobaltocene has been reported.[29−32] Other than this, one-electron oxidation reactions of alkyl halides with a high-spin Co(II) species or with an isolable Co(II) compound that contains a cobalt−carbon σ-bond would appear to be unknown.[33] We have prepared high- and low-spin cobalt(II) complexes and here report their reaction with alkyl halides, the structure of the resulting five-coordinate cobalt(III) complexes, and their utility for alkyl radical generation.

Results and Discussion

Synthesis and Structure of CoR[N(SiMe$_2$CH$_2$PPh$_2$)$_2$] (R = alkyl) Complexes. Addition of 1 equiv of LiN(SiMe$_2$CH$_2$PPh$_2$)$_2$ to a THF suspension of CoX_2 (X = Cl, Br) results in the rapid formation of a dark blue solution from which blue crystals of CoX[N(SiMe$_2$CH$_2$PPh$_2$)$_2$] (X = Cl, **1**; X = Br, **2**) can be isolated in high yield (eq 2).

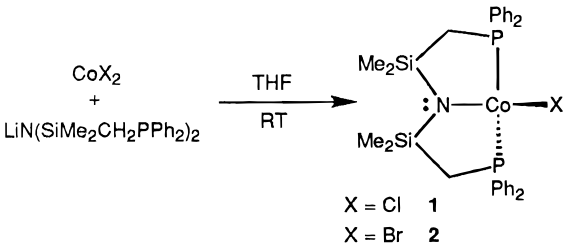

(2)

Solution magnetic moment measurements (Evans method)[34] showed a value of $\mu_{eff} = 4.2 \pm 0.1\ \mu_B$ for the halide derivatives, consistent with a high-spin tetrahedral Co(II) complex with some second-order orbital angular momentum contribution to the moment (spin-only d^7 is 3.89 μ_B).[35] The dark, intense blue color is also consistent with most high-spin tetrahedral Co(II) complexes;[36−38] the visible spectrum of **1** shows three bands at 506, 602, and 786 nm which shift to 518, 616, and 792 nm for the bromide **2**. An X-ray crystal structure of the iodide complex CoI[N(SiMe$_2$CH$_2$PPh$_2$)$_2$] (preparation is discussed later) was determined (see Supporting Information) and reveals a distorted tetrahedral geometry as expected. Variable-temperature magnetic susceptibility measurements from 4.2 to 80 K have also been carried out (see Supporting Information) and show a large D of 20 ± 1 cm^{-1} for the zero-field splitting of the ground $S = {}^3/_2$ state (d,[7] Co(II)).

Scheme 1

$$L_nM(II) + RX \longrightarrow L_nM(III)X + R\bullet$$
$$L_nM(II) + R\bullet \longrightarrow L_nM(III)R$$
$$2\,L_nM(II) + RX \longrightarrow L_nM(III)R + L_nM(III)X$$

The chloride derivative **1** is a convenient starting material for the synthesis of a variety of Co(II) alkyl compounds. Reaction of **1** with organolithium, sodium, or potassium reagents in THF or toluene forms the desired CoR[N(SiMe$_2$CH$_2$PPh$_2$)$_2$] complexes in moderate to high yield by salt metathesis. Specifically, reaction of **1** with MeLi, $PhCH_2K$, $LiCH_2SiMe_3$, and NaC_5H_5·DME yields the expected Co(II) alkyl complexes (**4**−**7**), as shown in eq 3. The Co(II) alkyls produced are all yellow-orange compounds, in stark contrast to the intense blue precursor **1**.

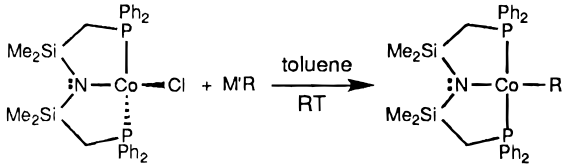

(3)

M'R = MeLi, MeMgBr **4**
M'R = KCH_2Ph **5**
M'R = $LiCH_2SiMe_3$ **6**
M'R = NaC_5H_5·DME **7**

The color change is an indication of the geometry and spin-state change that occurs upon halide for alkyl metathesis. The solution room-temperature magnetic moments for the Co(II) alkyls range from 1.9 to 2.2 μ_B, consistent with a low-spin d^7 center (one unpaired electron) with some second-order spin−orbit coupling.[35] This confirms that a geometry change from tetrahedral to square planar has occurred. It should be noted that the geometry of the cyclopentadienyl complex **7** is in fact unknown and could either have a distorted pseudotetrahedral structure with the cyclopentadienyl η^5 or a square planar geometry with an η^1 Cp group; nevertheless, a magnetic moment of 1.9 μ_B for **7** is indicative of a spin state change to low spin.

The X-ray crystal structure of Co(CH_2Ph)[N(SiMe$_2$CH$_2$PPh$_2$)$_2$] (**5**) is shown in Figure 1. Crystal data are collected in Table 1 and selected bond lengths and angles in Tables 2 and 3. The structural analysis confirms that cobalt benzyl **5** is

(22) Farmery, K.; Busch, D. H. *Inorg. Chem.* **1972**, *11*, 2901.
(23) Tyler, D. R. *Prog. Inorg. Chem.* **1988**, *36*, 125.
(24) Schneider, P. W.; Phelan, P. F.; Halpern, J. *J. Am. Chem. Soc.* **1969**, *91*, 77.
(25) Blaser, H.-U.; Halpern, J. *J. Am. Chem. Soc.* **1980**, *102*, 1684.
(26) Chock, P. B.; Halpern, J. *J. Am. Chem. Soc.* **1969**, *91*, 582.
(27) Halpern, J.; Maher, J. P. *J. Am. Chem. Soc.* **1964**, *86*, 2311.
(28) Halpern, J.; Maher, J. P. *J. Am. Chem. Soc.* **1965**, *87*, 5361.
(29) Herberich, G. E.; Bauer, E.; Schwarzer, J. *J. Organomet. Chem.* **1969**, *17*, 445.
(30) Herberich, G. E.; Bauer, E. *J. Organomet. Chem.* **1969**, *16*, 301.
(31) Herberich, G. E.; Schwarzer, J. *J. Organomet. Chem.* **1972**, *34*, C43.
(32) Herberich, G. E.; Carstensen, T.; Klein, W.; Schmidt, M. U. *Organometallics* **1993**, *12*, 1439.
(33) Reduction of RCo(III) complexes to Co(I) species, followed by reaction with RX to yield $R_2Co(III)$ systems, could proceed through in situ RCo(II) intermediates. See: Murakami, Y.; Hisaeda, Y.; Fan, S.-D.; Matsuda, Y. *Bull. Chem. Soc. Jpn.* **1989**, *62*, 2219. Elliott, C. M.; Hershenhart, E.; Finke, R. G.; Smith, B. L. *J. Am. Chem. Soc.* **1981**, *103*, 5558. Finke, R. G.; Smith, B. L.; Droege, M. W.; Elliott, C. M.; Hershenhart, E. *J. Organomet. Chem.* **1980**, *202*, C25. Costa, G.; Mestroni, G.; Cocevar, C. *J. Chem. Soc., Chem. Commun.* **1971**, 706. Costa, G.; Puxeddu, A.; Reisenhofer, E. *J. Chem. Soc., Chem. Commun.* **1971**, 993. Coleman, W. M.; Taylor, L. T. *J. Am. Chem. Soc.* **1971**, *93*, 5446.
(34) Sur, S. K. *J. Magn. Reson.* **1989**, *82*, 169.
(35) Carlin, R. L. *Magnetochemistry*; Springer-Verlag: Heidelberg, 1986.
(36) Cotton, F. A.; Faut, O. D.; Goodgame, D. M. L.; Holm, R. H. *J. Am. Chem. Soc.* **1961**, *83*, 1780.
(37) Cotton, F. A.; Wilkinson, G. *Advanced Inorganic Chemistry;* 5th ed.; John Wiley & Sons: New York, 1988.
(38) Horrocks, W. D.; Hecke, G. R. V.; Hall, D. D. *Inorg. Chem.* **1967**, *6*, 694.

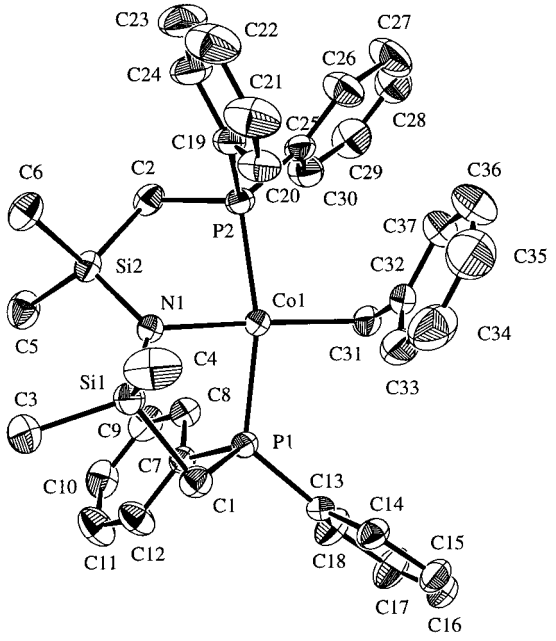

Figure 1. Molecular structure and numbering scheme for $Co(CH_2Ph)[N(SiMe_2CH_2PPh_2)_2]$ (**5**); 33% probability thermal ellipsoids are shown.

monomeric and square planar. There is some distortion from planarity in benzyl **5** as the two trans angles, P(1)−Co-P(2) and N−Co−C(31), are 162.93(3)° and 173.6(1)° (180° is ideal).

Other structurally characterized compounds[39] with Co(II)−C bonds include the cobalt(II) aryl complexes $Co(PEt_2Ph)_2(mesityl)_2$[40−42] and bis(μ-mesityl)dimesityldicobalt(II),[43] which are low-spin square planar and high-spin trigonal, respectively, with Co−C(sp^2) distances of 1.994(3) and 1.988(7) Å. A series of bulky cobalt alkyls stabilized by TMEDA have also been recently reported;[44] these are high-spin and tetrahedral, with Co−C distances ranging from 2.025(7) to 2.151(8) Å. In comparison, the Co−C bond length of 2.009 Å in **5** is shorter than that in the high-spin alkyls but not as short as for the low-spin, but stronger, aryl bond; this is rationalized by the smaller size of a low-spin Co(II) center vs the high-spin case. Similarly, the Co−P bond length is sensitive to spin state, as has been observed with other metal−phosphine systems.[45,46] A typical high-spin Co(II)−P bond length is 2.373(3) Å in **3** and 2.384(1) Å in $Co(PPh_3)_2X_2$.[47] Low-spin Co(II)−P bond lengths are substantially shorter, as observed in $Co(PEt_2Ph)_2(mesityl)_2$ (2.232(4) Å)[41,42] and herein for $Co(CH_2Ph)[N(SiMe_2CH_2PPh_2)_2]$ (**5**) (2.2127(8) and 2.2162(8) Å).

The known Co(II) silylamide complexes are all high-spin complexes and have Co−N bond lengths ranging from 1.898(3) and 1.904(3) Å (i.e., $Co[N(SiMePh_2)_2]_2$)[48] to 1.931(14) and 1.924(13) Å in $Co[N(SiMe_3)_2]_2PPh_3$.[49] In **5** the Co−N distance of 1.982(2) Å is longer than that observed for any other examples of cobalt(II) silylamide complexes. In addition the Si−N bond lengths of 1.702(2) and 1.707(2) Å in **5** are generally shorter than those found in other examples, for which a range of 1.710−1.785 Å is observed.

It is interesting to compare cobalt benzyl **5** to the chromium analogue, $Cr(CH_2Ph)[N(SiMe_2CH_2PPh_2)_2]$, which contains the exact same ligand set and overall geometry.[45] The most striking difference is that the electron-deficient chromium complex (12-electron system) binds the benzyl group in an η^2-fashion. On the other hand, in the more electron-rich 15-electron cobalt system the benzyl group is η^1-bound, as evidenced by the Co−C(31)−C(32) bond angle of 100.1(2)°.

Despite the fact that the cobalt(II) alkyl complexes are paramagnetic, ^{1}H NMR spectra can be observed.[50] As an example, the ^{1}H NMR spectrum of $CoMe[N(SiMe_2CH_2PPh_2)_2]$ (**4**) has five peaks present; the Co−CH_3 peak is not observed. The assignments are based on integration (60 °C spectrum,

Table 1. Crystallographic Data

compd	**5**[a]	**10**·0.5C_7H_8[a]
formula	$C_{37}H_{43}CoNP_2Si_2$	$C_{33.5}H_{40}Br_2CoNP_2Si_2$
fw	678.81	793.55
color, habit	red, prism	red, irregular
crystal size, mm	0.15 × 0.33 × 0.40	0.20 × 0.35 × 0.50
crystal system	triclinic	triclinic
space group	$P\bar{1}$ (No. 2)	$P\bar{1}$ (No. 2)
a, Å	10.6832(9)	11.759(2)
b, Å	16.877(1)	16.052(2)
c, Å	10.134(1)	9.853(2)
α, deg	97.830(8)	91.20(1)
β, deg	93.810(8)	98.43(1)
γ, deg	87.058(6)	97.59(1)
V, Å^3	1804.5(3)	1822.0(4)
Z	2	2
T, °C	21	21
ρ_{calc}, g/cm^3	1.249	1.446
F(000)	714	806
radiation	Mo	Cu
μ, cm^{-1}	6.51	78.97
transmission factors	0.93−1.00	0.56−1.00
scan type	$\omega-2\theta$	$\omega-2\theta$
scan range, deg in ω	1.00 + 0.35 tan θ	0.94 + 0.20 tan θ
scan speed, deg/min	16 (up to 9 scans)	16 (up to 9 scans)
data collected	$+h, \pm k, \pm l$	$+h, \pm k, \pm l$
$2\theta_{max}$, deg	60	120
crystal decay, %	3.6	negligible
total no. of reflns	11036	5475
no. of unique reflns	10504	5221
R_{merge}	0.034	0.056
no. with $I \geq n\sigma(I)$	4763	3527
no. of variables	389	389
R^c	0.035	0.039
R_w	0.030	0.042
gof[c]	1.66	0.91
max Δ/σ	0.001	0.005
residual density, e/Å^3	−0.25, 0.28	−0.43, 0.47

[a] Rigaku AFC6S diffractometer, takeoff angle 6.0°, aperture 6.0 × 6.0 mm at a distance of 285 mm from the crystal, stationary background counts at each end of the scan (scan/background time ratio 2:1), Cu Kα (λ = 1.54178 Å) or Mo Kα radiation (λ = 0.71069 Å), graphite monochromator, $\sigma^2(F^2) = [S^2(C + 4B)]/Lp^2$ (S = scan speed, C = scan count, B = normalized background count), function minimized $\sum w(|F_o| - |F_c|)^2$, where $w = 1$ for **10** and $w = 4F_o^2/\sigma^2(F_o^2)$ for **5**, $R = \sum||F_o| - |F_c||/\sum|F_o|$, $R_w = (\sum w(|F_o| - |F_c|)^2/\sum w|F_o|^2)^{1/2}$, and gof = $[\sum w(|F_o| - |F_c|)^2/(m-n)]^{1/2}$. Values given for R, R_w, and gof are based on those reflections with $I \geq 3\sigma(I)$.

(39) Allen, F. H.; Kennard, O.; Taylor, R. *Acc. Chem. Res.* **1983**, *16*, 146.
(40) Chatt, J.; Shaw, B. L. *J. Chem. Soc.* **1961**, 285.
(41) Falvello, L.; Gerloch, M. *Acta Crystallogr. B* **1979**, *B35*, 2547.
(42) Owston, P. G.; Rowe, J. M. *J. Chem. Soc.* **1963**, 3411.
(43) Theopold, K. H.; Silverstre, J.; Byrne, E. K.; Richeson, D. S. *Organometallics* **1989**, *8*, 2001.
(44) Hay-Motherwell, R. S.; Wilkinson, G.; Hussain, B.; Hursthouse, M. B. *Polyhedron* **1990**, *9*, 931.
(45) Fryzuk, M. D.; Leznoff, D. B.; Rettig, S. J. *Organometallics* **1995**, *14*, 5193.
(46) Hermes, A. R.; Morris, R. J.; Girolami, G. S. *Organometallics* **1988**, *7*, 2372.
(47) Carlin, R. L.; Chirico, R. D.; Sinn, E.; Mennenga, G.; Jongh, L. J. d. *Inorg. Chem.* **1982**, *21*, 2218.
(48) Bartlett, R. A.; Power, P. P. *J. Am. Chem. Soc.* **1987**, *109*, 7563.
(49) Bradley, D. C.; Hursthouse, M. B.; Smallwood, R. J.; Welch, A. J. *J. Chem. Soc., Chem. Commun.* **1973**, 872.
(50) Lamar, G. N.; Horrocks, W. D.; Holm, R. H. *NMR of Paramagnetic Molecules*; Academic Press: New York, 1973.

Table 2. Selected Bond Lengths (Å) for the Complexes $Co(CH_2Ph)[N(SiMe_2CH_2PPh_2)_2]$ (**5**) and $CoBr_2[N(SiMe_2CH_2PPh_2)_2]$ (**10**)

$Co(CH_2Ph)[N(SiMe_2CH_2PPh_2)_2]$ (**5**)			
Co(1)−P(1)	2.2127(8)	Co(1)−P(2)	2.2162(8)
Co(1)−N(1)	1.982(2)	Co(1)−C(31)	2.009(3)
P(1)−C(1)	1.808(3)	P(1)−C(7)	1.822(3)
P(1)−C(13)	1.830(3)	P(2)−C(2)	1.819(3)
P(2)−C(19)	1.827(3)	P(2)−C(25)	1.830(3)
Si(1)−N(1)	1.707(2)	Si(1)−C(1)	1.895(3)
Si(1)−C(3)	1.872(3)	Si(1)−C(4)	1.862(4)
Si(2)−N(1)	1.702(2)	Si(2)−C(2)	1.890(3)
Si(2)−C(5)	1.877(3)	Si(2)−C(6)	1.870(3)
C(31)−C(32)	1.480(4)		
$CoCl_2[N(SiMe_2CH_2PPh_2)_2]$ (**10**)			
Co(1)−Br(1)	2.375(1)	Co(1)−Br(2)	2.378(1)
Co(1)−P(1)	2.264(2)	Co(1)−P(2)	2.282(2)
Co(1)−N(1)	1.926(5)	P(1)−C(1)	1.798(6)
P(1)−C(7)	1.814(6)	P(1)−C(13)	1.810(6)
P(2)−C(2)	1.792(7)	P(2)−C(19)	1.827(6)
P(2)−C(25)	1.820(6)	Si(1)−N(1)	1.734(5)
Si(1)−C(1)	1.888(7)	Si(1)−C(3)	1.862(8)
Si(1)−C(4)	1.864(8)	Si(2)−N(1)	1.721(5)
Si(2)−C(2)	1.888(6)	Si(2)−C(5)	1.852(8)
Si(2)−C(6)	1.863(8)		

Table 3. Selected Bond Angles (deg) for the Complexes $Co(CH_2Ph)[N(SiMe_2CH_2PPh_2)_2]$ (**5**) and $CoBr_2[N(SiMe_2CH_2PPh_2)_2]$ (**10**)

$Co(CH_2Ph)[N(SiMe_2CH_2PPh_2)_2]$ (**5**)			
P(1)−Co(1)−P(2)	162.93(3)	P(1)−Co(1)−N(1)	82.83(6)
P(1)−Co(1)−C(31)	95.55(9)	P(2)−Co(1)−N(1)	86.98(6)
P(2)−Co(1)−C(31)	96.01(9)	N(1)−Co(1)−C(31)	173.6(1)
Co(1)−P(1)−C(1)	106.94(9)	Co(1)−P(1)−C(7)	108.10(9)
Co(1)−P(1)−C(13)	124.89(9)	C(1)−P(1)−C(7)	106.2(1)
C(1)−P(1)−C(13)	107.7(1)	C(7)−P(1)−C(13)	101.6(1)
Co(1)−P(2)−C(2)	101.58(10)	Co(1)−P(2)−C(19)	117.0(1)
Co(1)−P(2)−C(25)	121.62(9)	C(2)−P(2)−C(19)	104.3(1)
C(2)−P(2)−C(25)	106.4(1)	C(19)−P(2)−C(25)	104.1(1)
N(1)−Si(1)−C(1)	105.1(1)	N(1)−Si(1)−C(3)	114.4(1)
N(1)−Si(1)−C(4)	112.8(1)	C(1)−Si(1)−C(3)	108.6(1)
C(1)−Si(1)−C(4)	107.9(2)	C(3)−Si(1)−C(4)	107.8(2)
N(1)−Si(2)−C(2)	104.5(1)	N(1)−Si(2)−C(5)	113.8(1)
N(1)−Si(2)−C(6)	114.3(1)	C(2)−Si(2)−C(5)	108.2(1)
C(2)−Si(2)−C(6)	108.9(1)	C(5)−Si(2)−C(6)	106.8(1)
Co(1)−N(1)−Si(1)	115.2(1)	Co(1)−N(1)−Si(2)	118.5(1)
Si(1)−N(1)−Si(2)	126.3(1)	Co(1)−C(31)−C(32)	100.1(2)
$CoCl_2[N(SiMe_2CH_2PPh_2)_2]$ (**10**)			
Br(1)−Co(1)−Br(2)	117.88(5)	Br(1)−Co(1)−P(1)	91.18(5)
Br(1)−Co(1)−P(2)	88.92(5)	Br(1)−Co(1)−N(1)	121.4(2)
Br(2)−Co(1)−P(1)	88.41(6)	Br(2)−Co(1)−P(2)	96.96(6)
Br(2)−Co(1)−N(1)	120.7(1)	P(1)−Co(1)−P(2)	173.87(8)
P(1)−Co(1)−N(1)	87.7(1)	P(2)−Co(1)−N(1)	87.0(1)
Co(1)−P(1)−C(1)	103.5(2)	Co(1)−P(1)−C(7)	113.8(2)
Co(1)−P(1)−C(13)	119.8(2)	C(1)−P(1)−C(7)	106.9(3)
C(1)−P(1)−C(13)	109.0(3)	C(7)−P(1)−C(13)	103.2(3)
Co(1)−P(2)−C(2)	100.3(2)	Co(1)−P(2)−C(19)	120.1(2)
Co(1)−P(2)−C(25)	118.6(2)	C(2)−P(2)−C(19)	105.6(3)
C(2)−P(2)−C(25)	110.4(3)	C(19)−P(2)−C(25)	101.1(3)
N(1)−Si(1)−C(1)	105.5(2)	N(1)−Si(1)−C(3)	113.2(3)
N(1)−Si(1)−C(4)	113.0(3)	C(1)−Si(1)−C(3)	111.1(3)
C(1)−Si(1)−C(4)	106.7(3)	C(3)−Si(1)−C(4)	107.3(4)
N(1)−Si(2)−C(2)	104.5(3)	N(1)−Si(2)−C(5)	113.9(3)
N(1)−Si(2)−C(6)	112.4(3)	C(2)−Si(2)−C(5)	106.9(4)
C(2)−Si(2)−C(6)	110.7(3)	C(5)−Si(2)−C(6)	108.2(4)
Co(1)−N(1)−Si(1)	116.1(3)	Co(1)−N(1)−Si(2)	118.6(3)
Si(1)−N(1)−Si(2)	125.1(3)		

C_6D_6), the direction of shifting peaks upon increased temperature (peaks shift toward their diamagnetic values), and the inherent broadness of each peak (protons closer to the metal are broader).[51] The Si*Me*$_2$ peak at −3.3 ppm is easily identified by its unique integration (12H). Although the phenyl ortho and meta protons have the same integration (8H), the ortho protons (closer to the metal center) at 9.8 ppm are very broad (1.7 ppm width at half-height), much broader than the meta protons at 6.5 ppm (0.2 ppm width at half-height). Similarly the para protons and the backbone methylenes (both integrate to 4H) can be distinguished by the fact that the para protons at 8.4 ppm are sharp while the much closer methylene protons are observed at −6.3 ppm (1.3 ppm width). $^{31}P\{^1H\}$ NMR spectra are not observed for any of the complexes presented.

Scheme 2

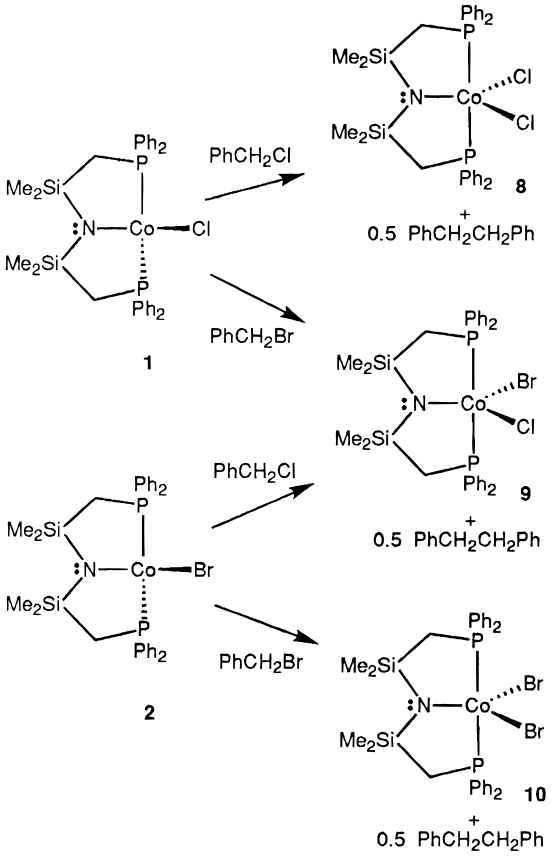

Reactivity of $CoX[N(SiMe_2CH_2PPh_2)_2]$ (X = Cl, Br) with Benzyl Halides. Addition of excess benzyl chloride (10 equiv) to a blue toluene solution of **1** results in a slow color change to bright red to generate the cobalt(III) complex $CoCl_2[N(SiMe_2CH_2PPh_2)_2]$ (**8**) (Scheme 2). Similarly, reaction of **1** with benzyl bromide rapidly progresses to give the mixed bromo−chloro derivative $CoBrCl[N(SiMe_2CH_2PPh_2)_2]$ (**9**). If this reaction is allowed to proceed over longer periods of time, a halide exchange reaction occurs to yield the dibromo complex $CoBr_2[N(SiMe_2CH_2PPh_2)_2]$ (**10**) and benzyl chloride (detected by ^1H NMR spectroscopy). This last step is substantially slower than the one-electron oxidation, but it makes obtaining pure **9** difficult. The dibromide **10** can also be made from $CoBr[N(SiMe_2CH_2PPh_2)_2]$ (**2**) and benzyl bromide; in this case the reaction proceeds to completion within 2 h. In all cases, the benzyl group ends up as 0.5 equiv of bibenzyl ($PhCH_2CH_2Ph$), detected by ^1H NMR spectroscopy (2.85 ppm) and by mass spectroscopy (*m*/*e* 182, M^+).

The intermediacy of benzyl radicals was substantiated by performing the reaction in the presence of the radical trapping agent, TEMPO. The benzyl-trapped product, *N*-benzyloxy-2,2,6,6-tetramethylpiperidine, was identified by MS (*m*/*e* 247, M^+) and by ^1H NMR spectroscopy (singlet at 4.82 ppm due to N−O−C*H*$_2$−Ph).[13] Control reactions showed that TEMPO

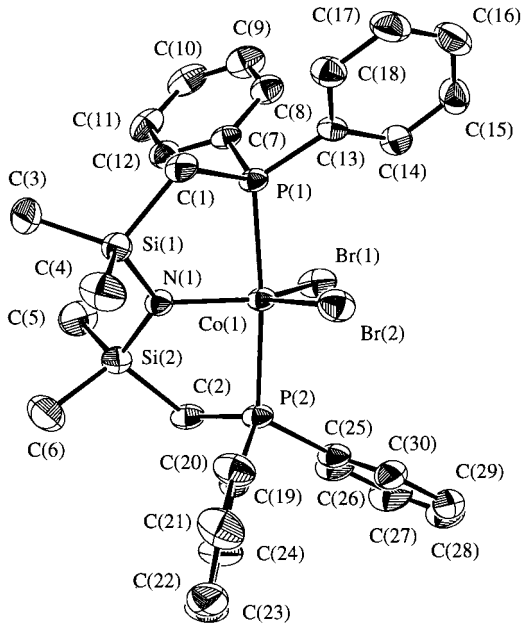

Figure 2. Molecular structure and numbering scheme for $CoBr_2[N(SiMe_2CH_2PPh_2)_2]$ (**10**); 33% probability thermal ellipsoids are shown.

does not react with $CoX[N(SiMe_2CH_2PPh_2)_2]$ or with benzyl halides separately.

Five-coordinate Co(III) complexes are not that common. The vast majority of Co(III) derivatives are octahedral and generally are diamagnetic (low spin d^6).[37] In contrast, complexes **8**, **9**, and **10** are paramagnetic, with solution magnetic moments of 3.6, 3.1, and 3.3 μ_B, respectively. A value of 3.1 μ_B for **9** is consistent with a d^6 intermediate spin system,[52] corresponding to two unpaired electrons, and is within the observed range of the other five-coordinate Co(III) complexes known. The observed value of 3.6 μ_B for **8**, however, is substantially higher; the reasons for this are uncertain.

Despite the paramagnetism of these complexes, broad, shifted ^1H NMR spectra can be observed and integration and variable-temperature NMR spectra yield chemical shift information. To our knowledge there is only one other cobalt(III) paramagnetic ^1H NMR spectrum reported.[53]

To confirm the nature of the coordination sphere, an X-ray crystal structure of **10** was obtained. The structural analysis reveals the nearly perfectly trigonal-bipyramidal geometry around cobalt (Figure 2). The phosphines are trans-axially oriented, with a P−Co−P angle of 173.87(8)° (Table 3). The amide and two halides are equatorial, with the in-plane angles of 117.88(5)°, 121.4(2)°, and 120.7(1)° an indication of the lack of distortion in this system. Note that an undistorted trigonal bipyramid is the theoretically predicted structure for a five-coordinate intermediate-spin d^6 complex; a low-spin d^6 complex such as $Ir(R)X[N(SiMe_2CH_2PPh_2)]$ will Jahn−Teller distort.[54−57]

Of the few structurally characterized examples of five-coordinate cobalt(III) complexes, the majority are square pyramidal, usually CoL_4X, where L_4 is a square-planar system such as porphyrin or salen and X is an alkyl or halide group.[58−64] Although most of these are diamagnetic, a few are paramagnetic with $\mu_{eff} = 2.4-3.25$ μ_B.[65−68] There are, to our knowledge, only three X-ray structures of trigonal-bipyramidal cobalt(III) complexes: $CoCl_3(PEt_3)_2$,[69] $CoI_3(PMe_3)_2$,[70] and $CoI_3(SbPh_3)_2$.[71] As well, a series of $CoX_3(PR_3)_2$ complexes have been studied spectroscopically and by EXAFS to yield structural information.[72,73] From the X-ray and EXAFS studies, Co−P bond lengths in trigonal-bipyramidal Co(III) complexes range from 2.28 to 2.34 Å; in comparison, the Co−P bond lengths in **10** of 2.264(2) and 2.282(2) Å are on the short side but otherwise unremarkable. As expected, the Co−P distances are sensitive to spin state; Co−P distances in diamagnetic octahedral Co(III) complexes such as $CoMe_2(PMe_3)_2(\mu\text{-}(CH_2)_2PMe_2)$ (2.196, 2.174 Å)[74] are significantly shorter than in **10**.

Cobalt(III) amides (excluding porphyrin-type macrocycles) are uncommon. The homoleptic amide, high-spin trigonal $Co[N(SiMe_3)_2]_3$, with Co−N and Si−N bond lengths of 1.870(3) and 1.754(2) Å, respectively, has been reported.[75] In **10** the Co−N distance of 1.926(5) Å and Si−N distances of 1.734(5) and 1.721(5) Å indicate a lesser degree of amide lone-pair interaction with the metal center.

Because of the scarcity of Co(III) compounds in a trigonal-bipyramidal geometry, there is a lack of detailed magnetic data for such systems. The $CoX_3(PR_3)_2$ series of complexes[69,70,72,73] are paramagnetic with $\mu_{eff} = 2.93-3.28$ μ_B, comparable to **9** and **10**, but $CoI_3(SbPh_3)_2$ has a room-temperature magnetic moment of 4.4 μ_B, possibly consistent with some spin-equilibrium process.[71] However, no detailed variable-temperature magnetic study of a trigonal-bipyramidal Co(III) system has been reported, either in the solid state or in solution.

The solid-state molar magnetic susceptibility (χ_m) of $CoBr_2[N(SiMe_2CH_2PPh_2)_2]\cdot(0.5\ C_7H_8)$ (**10**) was measured from 4.4 to 81.5 K and the results are shown in Figure 3 as a plot of magnetic moment vs temperature. At high temperatures the

(51) Muller, G.; Neugebauer, D.; Geike, W.; Kohler, F. H.; Pebler, J.; Schmidbaur, H. *Organometallics* **1983**, *2*, 257.
(52) Kahn, O. *Molecular Magnetism*; VCH: New York, 1993.
(53) Collins, T. J.; Richmond, T. G.; Santarsiero, B. D.; Treco, B. G. R. T. *J. Am. Chem. Soc.* **1986**, *108*, 2088.
(54) Jean, Y.; Eisenstein, O. *Polyhedron* **1988**, *7*, 405.
(55) Rachidi, I. E.-I.; Eisenstein, O.; Jean, Y. *New J. Chem.* **1990**, *14*, 671.
(56) Riehl, J. F.; Jean, Y.; Eisenstein, O.; Pelissier, M. *Organometallics* **1992**, *11*, 729.
(57) Fryzuk, M. D.; MacNeil, P. A.; Massey, R. L.; Ball, R. G. *J. Organomet. Chem.* **1989**, *368*, 231.
(58) Bruckner, S.; Calligaris, M.; Nardin, G.; Randaccio, L. *Inorg. Chim. Acta* **1969**, *3*, 308.
(59) Costa, G.; Mestroni, G.; Stefani, L. *J. Organomet. Chem.* **1967**, *7*, 493.
(60) Costa, G.; Mestroni, G.; Tauzher, G.; Stefani, L. *J. Organomet. Chem.* **1966**, *6*, 181.
(61) Hitchcock, P. B.; McLaughlin, G. M. *J. Chem. Soc., Dalton Trans.* **1976**, 1927.
(62) Jaynes, B. S.; Ren, T.; Masschelien, A.; Lippard, S. J. *J. Am. Chem. Soc.* **1993**, *115*, 5589.
(63) Marzilli, L. G.; Summers, M. F.; Bresciani-Pahor, N.; Zangrando, E.; Charland, J.-P.; Randaccio, L. *J. Am. Chem. Soc.* **1985**, *107*, 6880.
(64) Summers, J. S.; Petersen, J. L.; Stolzenberg, A. M. *J. Am. Chem. Soc.* **1994**, *116*, 7189.
(65) Bailey, N. A.; McKenzie, E. D.; Worthington, J. M. *J. Chem. Soc., Dalton Trans.* **1977**, 763.
(66) Gerloch, M.; Higson, B. M.; McKenzie, E. D. *J. Chem. Soc., Chem. Commun.* **1971**, 1149.
(67) König, E.; Kremer, S.; Schnakig, R.; Kanellakopulos, B. *Chem. Phys.* **1978**, *34*, 379.
(68) McKenzie, E. D.; Worthington, J. M. *Inorg. Chim. Acta* **1976**, *16*, 9.
(69) van Enckevort, W. K. P.; Hendricks, H. M.; Beurskens, P. T. *Cryst. Struct. Commun.* **1977**, *6*, 531.
(70) McAuliffe, C. A.; Godfrey, S. M.; Mackie, A. G.; Pritchard, R. G. *Angew. Chem., Int. Ed. Engl.* **1992**, *31*, 919.
(71) Godfrey, S. M.; McAuliffe, C. A.; Pritchard, R. G. *J. Chem. Soc., Chem. Commun.* **1994**, 45.
(72) Levason, W.; Ogden, J. S.; Spicer, M. D. *Inorg. Chem.* **1989**, *28*, 2128.
(73) Levason, W.; Spicer, M. D. *J. Chem. Soc., Dalton Trans.* **1990**, 719.
(74) Brauer, D. J.; Kruger, C.; Roberts, P. J.; Tsay, Y.-H. *Chem. Ber.* **1974**, *107*, 3706.
(75) Ellison, J. J.; Power, P. P.; Shoner, S. C. *J. Am. Chem. Soc.* **1989**, *111*, 8044.

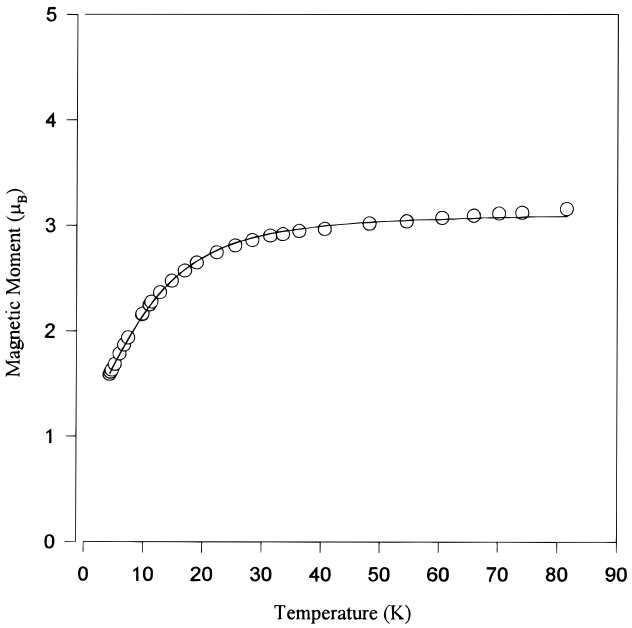

Figure 3. Graph of magnetic susceptibility vs T for $CoBr_2[N(SiMe_2CH_2PPh_2)_2]$ (**10**).

magnetic moment tends toward the 3.3 μ_B observed at room temperature, consistent with some second-order spin−orbit coupling to an intermediate-spin d^6 $S = 1$ system. As the temperature is lowered the moment drops to 1.59 μ_B at 4.4 K, a behavior that may be attributed to zero-field splitting (ZFS) of the $S = 1$ level into the ± 1 Kramers doublet and a nonmagnetic $S = 0$ state, with a separation of D cm^{-1}. The data were analyzed with use of the equation for zero-field splitting of a $S = 1$ state,[76]

$$\chi_{Co(III)} = {}^1/_3\left[C\frac{2e^{-x}}{1+2e^{-x}}\right] + {}^2/_3\left[C\frac{(2/x)(1-e^{-x})}{1+2e^{-x}}\right]$$

where $C = (Ng^2\mu_\beta{}^2/kT)$ and $x = (D/kT)$. The experimental data could be accurately fit to the model by the inclusion of a small amount of paramagnetic $S = {}^3/_2$ impurity, likely the Co(II) starting material. This was accomplished by combining the above expression with the Curie law term,

$$\chi_{para} = \frac{Ng^2\mu_\beta{}^2S(S+1)}{3kT}$$

according to,

$$\chi_m = [1-P]\chi_{Co(III)} + P\chi_{para}$$

where P represents the fraction of paramagnetic impurity ($g = 2.3$). The fit was achieved via a nonlinear least-squares procedure, using a minimized goodness of fit function F; the best fit of the experimental data with theory (Figure 3) yields $D = 32.6 \pm 0.5$ cm^{-1}, $g = 2.15 \pm 0.006$, and $P = 0.0523 \pm 0.003$ ($F = 0.0159$). A negative value of D was not fit adequately to the model, implying that the positive sign of D is valid. A change in the g-value of the paramagnetic impurity from 2.15 to 2.3 did not change the D or g value of the fit, but merely the amount of paramagnetic impurity P. The splitting value of 32.6 cm^{-1} is quite large, but as mentioned previously, there is a paucity of data on trigonal-bipyramidal Co(III) systems with which to compare this value. The $S = 1$ intermediate spin state has been observed in square-planar and square-pyramidal Co(III) complexes and the zero-field splitting parameter has been measured in a square-planar $K[Co^{III}N_4]\cdot 2H_2O$ system (N_4 = tetradentate diaminodiamido ligand) to be 53.7 cm^{-1}.[77,78] Variable-temperature measurements on square-planar $[{}^tBu_3N][Co(NS)_2]$ (NS = aminothiophenolato ligand) were not conducted to low enough temperature to measure the zero-field splitting.[79] A series of square-pyramidal Co(III) complexes, $Co(III)N_4X$ (N_4 = tetradentate diaminodiamido ligand; X = Cl, Br, I), were investigated in detail; the magnetism was found to be particularly complex and no zero-field splittings were reported.[66,67] Square-planar Fe(II) phthalocyanine is intermediate-spin and a zero-field splitting value of 69.9 cm^{-1} has been reported;[80] iron(II) tetraphenylporphyrin is also an intermediate-spin compound but its magnetic behavior is complicated by mixing of terms of similar energy.[81] Other metal centers which exhibit $S = 1$ zero-field splitting include high-spin d^8 Ni(II) complexes and d^2 V(III) complexes.[35,52] It would be interesting to be able to correlate zero-field splitting values for Co(III) with geometry and ligand field strength as has been done for high-spin Co(II) systems;[82−84] however, at present there are insufficient data in different geometries, although it does appear that square-planar coordination enforces greater zero-field splitting than a five-coordinate trigonal-bipyramidal geometry.

The UV−vis spectra of these Co(III) compounds are dominated by an intense band around 500 nm and another band around 330 nm. By using these bands, each dihalo derivative can be uniquely identified. Absorption spectra of CoX_3P_2 complexes have been extensively studied,[72,73,85,86] and on the basis of these similar compounds, the large band observed around 500 nm is assigned as a phosphine to metal ($P(\sigma)\rightarrow M(d_{xy,x^2-y^2})$) charge-transfer band; the extinction coefficient of 1770 M^{-1} cm^{-1} supports this assignment. Similarly, the higher energy band is assigned as a phosphine to metal ($P(\sigma)\rightarrow M(d_{z^2})$) charge-transfer band. An extra charge-transfer band in **10** at 434 nm is assigned as a bromine-to-metal ($Br(\pi)\rightarrow M(d_{xy,x^2-y^2})$) transition. One can observe d−d bands around 400−434 nm and also at lower energy, but these are much weaker in intensity and appear at best as shoulders, or are obscured completely.

Dramatic color changes and independent knowledge of spectra of complexes led UV−visible spectroscopy to become the method of choice for some preliminary kinetic investigations as well as compound identification. The reaction of $PhCH_2X$ (X = Cl, Br) and $CoY[N(SiMe_2CH_2PPh_2)_2]$ (Y = Cl, Br) was conveniently monitored by following the growth of the product $CoXY[N(SiMe_2CH_2PPh_2)_2]$ as evidenced by its absorption around 500 nm.

The effect of changing the halide on the bimolecular rate constant k of the reaction was probed by reaction of **1** with

(76) O'Connor, C. J. *Prog. Inorg. Chem.* **1982**, *29*, 203.
(77) König, E.; Schnakig, R.; Kanellakopulos, B. *J. Chem. Phys.* **1975**, *62*, 3907.
(78) Birker, P. J. M. W. L.; Bour, J. J.; Steggerda, J. J. *Inorg. Chem.* **1973**, *12*, 1254.
(79) Birker, P. J. M. W. L.; Boer, E. A. d.; Bour, J. J. *J. Coord. Chem.* **1973**, *3*, 175.
(80) Dale, B. W.; Williams, R. J. P.; Johnson, C. E.; Throp, T. L. *J. Chem. Phys.* **1968**, *49*, 3441.
(81) Nakazawa, H.; Yamaguchi, Y.; Mizuta, T.; Ichimura, S.; Miyoshi, K. *Organometallics* **1995**, *14*, 4635.
(82) Makinen, M. W.; Kuo, L. C.; Yim, M. B.; Wells, G. B.; Fukuyama, J. M.; Kim, J. E. *J. Am. Chem. Soc.* **1985**, *107*, 5245.
(83) Makinen, M. W.; Yim, M. B. *Proc. Natl. Acad. Sci. U.S.A.* **1981**, *78*, 6221.
(84) Carlin, R. L. *Science* **1985**, *227*, 1291.
(85) Jensen, K. A.; Jorgensen, C. K. *Acta Chem. Scand.* **1965**, *19*, 451.
(86) Jenson, K. A.; Nygaard, B.; Pedersen, C. T. *Acta Chem. Scand.* **1963**, *17*, 1126.

Scheme 3

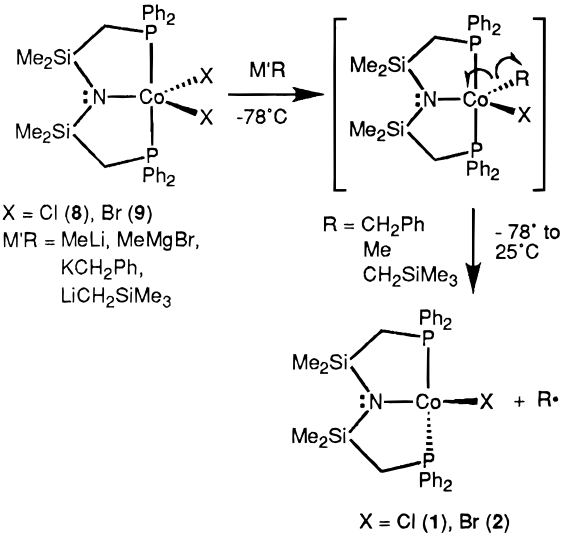

benzyl chloride and benzyl bromide (Scheme 2). Plots of k_{obs} vs [$PhCH_2X$] were linear under pseudo-first-order conditions, confirming the bimolecular nature of the reaction. Data give a rate constant of $k = 8.4 \pm 0.5 \times 10^{-5}$ M^{-1} s^{-1} for $PhCH_2Cl$ and $k = 1.6 \pm 0.5 \times 10^{-2}$ M^{-1} s^{-1} for $PhCH_2Br$ addition. The much faster rate for benzyl bromide, coupled with the observation of bibenzyl, supports the generally accepted radical-based mechanism for this type of reaction.[23,24,26,28,87−90] In addition, consistent with a radical-based mechanism, the reaction does not occur with unactivated substrates such as chlorobenzene.[91]

According to the classical mechanism shown in Scheme 1, the reaction of $PhCH_2X$ with a Co(II) complex should produce two products: a cobalt(III)−benzyl derivative and a Co(III)X complex. In the reaction being monitored above, this corresponds to $Co(CH_2Ph)X[N(SiMe_2CH_2PPh_2)]$ from alkyl transfer and $CoX_2[N(SiMe_2CH_2PPh_2)_2]$ from halide transfer. However, no evidence for the former compound was observed, either by NMR or by UV−vis spectroscopy. To test whether a five-coordinate, organocobalt(III) complex of the type $Co(R)X[N(SiMe_2CH_2PPh_2)_2]$ would be stable, we attempted to metathesize one halide of dichloride **8** with various alkylating agents to generate this putative species independently. Addition of 1 equiv of an alkyllithium or Grignard reagent (MeLi, $PhCH_2MgCl$, $LiCH_2SiMe_3$) to the dichloride, $CoCl_2[N(SiMe_2CH_2PPh_2)_2]$ (**8**), resulted in the formation of dark blue **1**, the Co(II) starting material, identified by its visible spectrum. Further addition of reagent formed the Co(II) alkyl species as would be expected. This result suggests that the five-coordinate Co(III) alkyls are intrinsically unstable and decompose upon formation by homolytic cleavage of the Co(III)−C bond to give a Co(II) product and the alkyl radical (Scheme 3). Attempts to stabilize the cobalt(III) alkyl halide complex by performing the reaction at lower temperatures were not successful; thus addition of alkyllithium reagents to $CoCl_2[N(SiMe_2CH_2PPh_2)_2]$ (**8**) at −78 °C caused a color change from red to yellow/orange, which upon warming turned to the blue color of the Co(II) species. This low-temperature color change may indeed be the intermediate alkyl halide complex, but this proved unisolable despite attempts at adding trapping agents (phosphine, pyridine, CO) at low temperature.

Scheme 4

$$CoX_2[N(SiMe_2CH_2PPh_2)_2] + RLi \longrightarrow CoRX[N(SiMe_2CH_2PPh_2)_2]$$

$$CoRX[N(SiMe_2CH_2PPh_2)_2] \longrightarrow CoX[N(SiMe_2CH_2PPh_2)_2] + R\bullet$$

$$R\bullet + PhCH_3 \longrightarrow RH + PhCH_2\bullet$$

$$2\ PhCH_2\bullet \longrightarrow PhCH_2CH_2Ph$$

With regard to the one-electron oxidation of $CoX[N(SiMe_2CH_2PPh_2)_2]$ by RX, the stoichiometry of this reaction is therefore 1:1, and not 1:0.5 as is found in classical systems (Scheme 1). This is due to the fact that alkyl radicals, R•, do not form stable complexes with the Co(II) present.[92] Facile homolysis of Co(III)−carbon bonds is well-known in the literature; macrocyclic ligands and/or the proper choice of base tend to stabilize these bonds.[93−96] Stable nonmacrocyclic alkyl complexes have been prepared but all are octahedral, diamagnetic, and therefore sterically and electronically saturated. Examples include $CoMe_3(PMe_3)_3$,[97] $CoR_2(acac)(PR'_3)_2$,[98] and CpCoLRR′.[99] Surprisingly, addition of triethylphosphine to the dihalo complexes **8** or **9** showed no change in either the ^1H NMR or UV−vis spectra and no alkyl species could be trapped by performing metathesis reactions in the presence of donor ligands. The stability of the five-coordinate, 16-electron complexes to neutral donor addition could be due to sterics, but an examination of the X-ray crystal structure of **10** suggests that such steric crowding is not present. A more likely explanation lies in the stability of the five-coordinate triplet state versus the six-coordinate state, which would have to undergo spin pairing to form a singlet state. Others have observed that in many situations,[100] in particular in 15-electron Cr(III) systems,[101] the addition of a donor ligand is insufficient to overcome the electronic cost of spin pairing, and despite electronic unsaturation at the metal, donor binding is not observed.

Monitoring the reaction of $LiCH_2SiMe_3$ with dichloride **8** in an NMR tube resulted in the formation of Me_4Si and $PhCH_2CH_2Ph$ (bibenzyl), presumably from a trimethylsilylmethyl radical ($Me_3SiCH_2\bullet$) abstracting a proton from the toluene solvent. The resulting benzyl radicals then coupled to form bibenzyl (Scheme 4). The observation of these products supports the intermediacy of alkyl radicals in this chemistry. This implies that complexes **8**−**10** can be used to generate alkyl radicals in situ given the appropriate organolithium or Grignard reagent.

(87) Huber, T. A.; Macartney, D. H.; Baird, M. C. *Organometallics* **1993**, *12*, 4715.
(88) Huber, T. A.; Macartney, D. H.; Baird, M. C. *Organometallics* **1995**, *14*, 592.
(89) Lee, K.-W.; Brown, T. L. *J. Am. Chem. Soc.* **1987**, *109*, 3269.
(90) Scott, S. L.; Espenson, J. H.; Zhu, Z. *J. Am. Chem. Soc.* **1993**, *115*, 1789.
(91) A complicating factor in the reaction of **1** with benzyl bromide is the slower ongoing chloride for bromide substitution reaction, i.e., conversion of **9** to **10**. To account for this potentially overlapping reaction kinetically, the reaction of **2** with benzyl bromide was also monitored. The rate constant for this reaction is $k = 2.0 \pm 0.5 \times 10^{-2}$ M^{-1} s^{-1}, implying that the halide exchange side-reaction does not greatly affect the overall kinetic data. Note that no peaks characteristic of dibromide **10** (e.g. the extra CT band at 434 nm) are observed in kinetic experiments starting with cobalt chloride **1**.
(92) It must be assumed on the basis of precedent that in fact the generated alkyl radicals do combine with the cobalt(II) halide complex present, but the resulting alkyl halide is homolytically unstable, releasing the alkyl radical back to the system.
(93) Bresciani-Pahor, N.; Forcolin, M.; Marzilli, L. G.; Randaccio, L.; Summers, M. F.; Toscano, P. J. *Coord. Chem. Rev.* **1985**, *63*, 1.
(94) Costa, G. *Pure Appl. Chem.* **1972**, *30*, 335.
(95) Ng, F. T. T.; Rempel, G. L. *J. Am. Chem. Soc.* **1982**, *104*, 621.
(96) Tsou, T.-T.; Loots, M.; Halpern, J. *J. Am. Chem. Soc.* **1982**, *104*, 623.
(97) Klein, H.-F.; Karsch, H. H. *Chem. Ber.* **1975**, *108*, 956.
(98) Ikariya, T.; Yamamoto, A. *J. Organomet. Chem.* **1976**, *116*, 239.
(99) Yamazaki, H.; Hagihara, N. *J. Organomet. Chem.* **1970**, *21*, 431.
(100) Poli, R. *Chem. Rev.* **1996**, *96*, 2135.
(101) Fettinger, J. C.; Mattamana, S. P.; Poli, R.; Rogers, R. D. *Organometallics* **1996**, *15*, 4211.

Reactivity of CoMe[N(SiMe$_2$CH$_2$PPh$_2$)$_2$] (4) with Alkyl Halides. Addition of 1 equiv of MeI to a yellow toluene solution of **4** results in the slow formation of a green solution with visible spectral bands at 538, 634, and 806 nm. This is similar to the bands of **1** and **2** and the product is identified by the visible spectrum, ^{1}H NMR spectrum, elemental analysis, and mass spectrum as CoI[N(SiMe$_2$CH$_2$PPh$_2$)$_2$] (**3**). Similarly, **2** can be prepared by addition of MeBr to **4** (eq 4).

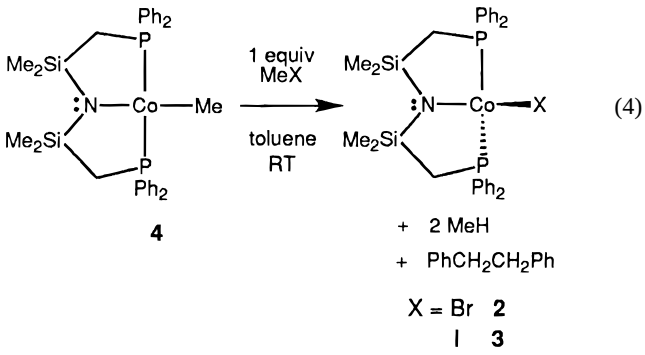

4 (4)

The final product, then, is still a Co(II) product; apparently a halide for alkyl metathesis has occurred and not an oxidation. This result is seemingly contrary to what one would expect, based on the classical mechanism. Thus, halide abstraction by the cobalt(II) alkyl **4** should be the first step, to give Co(Me)X[N(SiMe$_2$CH$_2$PPh$_2$)$_2$]; however, this complex was shown to rapidly decompose by Co−R bond homolysis to generate the observed product CoX[N(SiMe$_2$CH$_2$PPh$_2$)$_2$] and presumably methane from the methyl radical abstracting a proton from toluene (bibenzyl is also observed). As a result, one-electron oxidation chemistry *is* occurring, followed by a rapid one-electron reduction to yield the apparent halide for alkyl substitution.

Addition of approximately 1 equiv of benzyl chloride to **4** gives two products over several hours, their proportions depending on the relative concentration of **4** and PhCH$_2$X. One product is **1**, the halide for alkyl metathesis product. A second, minor product precipitates out of toluene as a purple powder. If the reaction is done in excess benzyl chloride, after the formation of **1**, the reaction continues on to form **8**, the halide transfer product, but this step is slow enough that the formation of **1** is readily observable. That is not the case for benzyl bromide addition, where the primary product CoBr[N(SiMe$_2$CH$_2$PPh$_2$)$_2$] (**2**) rapidly continues reacting with benzyl bromide to give CoBr$_2$[N(SiMe$_2$CH$_2$PPh$_2$)$_2$] (**10**), both identified by UV−visible spectroscopy. In this reaction, over time, a purple powder also precipitates out of solution. These minor purple products and the mechanism of their formation will be presented elsewhere.[102]

To determine the fate of the alkyl group on the cobalt in the case of halide-for-alkyl substitution, the reaction of Co(CH$_2$SiMe$_3$)[N(SiMe$_2$CH$_2$PPh$_2$)$_2$] (**6**) with excess benzyl bromide was followed by ^{1}H NMR spectroscopy. In the presence of excess benzyl bromide, the formation of Me$_3$SiCH$_2$Br was clearly observed along with bibenzyl. The presence of trimethylsilylmethyl bromide can be attributed to the formation of Me$_3$SiCH$_2^{\bullet}$ radicals, which can abstract a bromide from the excess benzyl bromide present. This result also illustrates the inherent instability of the corresponding Co(III) complex, Co(CH$_2$SiMe$_3$)Br[N(SiMe$_2$CH$_2$PPh$_2$)$_2$], which must decompose by rapid homolysis of the cobalt−carbon bond, as shown in other experiments. In addition, if the reaction of **4** with benzyl chloride is conducted in a sealed NMR tube, bibenzyl is produced and peaks assignable to **1** are observed.

(102) Fryzuk, M. D.; Leznoff, D. B.; Young, V. G., Jr. Manuscript in preparation.

Conclusions

The results of this study show that one-electron oxidation of Co(II) to Co(III) by certain alkyl halides is dependent on both the ancillary ligands and the spin state of the complex. Rather than observe the typical products found for the classical mechanism (Scheme 1), the halide complexes CoX[N(SiMe$_2$CH$_2$PPh$_2$)$_2$] react with 1 equiv of RX to generate the corresponding trivalent derivatives CoX$_2$[N(SiMe$_2$CH$_2$PPh$_2$)$_2$]. The reaction of square-planar, low-spin CoR[N(SiMe$_2$CH$_2$PPh$_2$)$_2$] complexes with 1 equiv of RX gives their precursor CoX[N(SiMe$_2$CH$_2$PPh$_2$)$_2$] complexes. While the mechanism of the activation of alkyl halides by these Co(II) derivatives no doubt follows that proposed for the classical mechanism, the instability of the presumed cobalt(III) alkyl derivative, Co(R)X[N(SiMe$_2$CH$_2$PPh$_2$)$_2$], one of the putative products of this reaction, is the key to the nonclassical outcome of these reactions. Hence, this leads to a change in the stoichiometry of the process; instead of 0.5 equiv of RX, 1 equiv of the alkyl halide must be used. Further confirmation of the unstable nature of the five-coordinate, Co(III) alkyl halide complexes was obtained by reaction of organolithium reagents, RLi, with the stable cobalt(III) derivative, CoX$_2$[N(SiMe$_2$CH$_2$PPh$_2$)$_2$]; reduction to Co(II) was observed along with products found, indicative of the presence of alkyl radical, R$^{\bullet}$.

The trivalent, five-coordinate cobalt complexes CoX$_2$[N(SiMe$_2$CH$_2$PPh$_2$)$_2$] are paramagnetic and show variable-temperature magnetic behavior consistent with $S = 1$ zero-field splitting. To our knowledge, this represents the first detailed magnetic study of a trigonal-bipyramidal Co(III) derivative.

Experimental Section

General Procedures. Unless otherwise stated all manipulations were performed under an atmosphere of dry, oxygen-free dinitrogen or argon by means of standard Schlenk or glovebox techniques. The glovebox used was a Vacuum Atmospheres HE-553-2 workstation equipped with a MO-40-2H purification system and a −40 °C freezer. ^{1}H NMR spectroscopy was performed on a Bruker WH-400 or a Bruker AC-200 instrument operating at 400 and 200 MHz, respectively. ^{1}H NMR spectra were referenced to internal C$_6$D$_5$H (7.15 ppm). Magnetic moments were measured by a modification of Evans Method (C$_6$D$_5$H as a reference peak) on the NMR spectrometers listed above. Infrared spectra were recorded on a BOMEM MB-100 spectrometer. UV−Vis spectra were recorded on a HP-8452A diode array spectrophotometer. Mass spectra were measured with a Kratos MS-50 EI instrument operating at 70 eV. Microanalyses (C, H, N) were performed by Mr. P. Borda of this department.

Materials. The preparation of the lithium salt LiN(SiMe$_2$CH$_2$PPh$_2$)$_2$ has been previously described.[103] NaCp·DME was prepared by the reaction of Na with CpH in dry DME. KCH$_2$Ph and LiCH$_2$SiMe$_3$ were prepared by literature procedures.[104] CoCl$_2$ and CoBr$_2$ were either used as received or dried in refluxing Me$_3$SiCl. Alkyl halides were either distilled under N$_2$ or passed through a column of activated alumina, and then degassed by 3 freeze−pump−thaw cycles. All other reagents were obtained from commercial sources and used as received.

Hexanes, toluene, and THF were heated to reflux over CaH$_2$ prior to a final distillation from either sodium metal or sodium benzophenone ketyl under an Ar atmosphere. Deuterated solvents were dried by distillation from sodium benzophenone ketyl under nitrogen; oxygen was removed by trap-to-trap distillation and 3 freeze−pump−thaw cycles.

(103) Fryzuk, M. D.; MacNeil, P. A.; Rettig, S. J.; Secco, A. S.; Trotter, J. *Organometallics* **1982**, *1*, 918.

(104) Schlosser, M.; Ladenberger, V. *J. Organomet. Chem.* **1967**, *8*, 193.

Variable-Temperature Magnetic Susceptibility Measurements. Magnetic susceptibility measurements on powdered samples of iodide **3** (see Supporting Information) and dibromide **10** were made at an applied field of 7500 G over the temperature range 4.6 to 80 K with a PAR Model 155 vibrating-sample magnetometer as previously described.[105] Magnetic susceptibilities were corrected for the diamagnetism of all atoms with Pascal's constants.

X-ray Crystallographic Analyses. $Co(CH_2Ph)[N(SiMe_2CH_2PPh_2)_2]$ (5) and $CoBr_2[N(SiMe_2CH_2PPh_2)_2]$ (10)·0.5C_7H_8. For complexes **5** and **10**, crystallographic data appear in Table 1. The final unit-cell parameters were obtained by least squares on the setting angles for 25 reflections with $2\theta = 22.0-31.7°$ for **5** and 19.1−57.5° for **10**. The intensities of three standard reflections, measured every 200 reflections, decayed linearly by 3.6% for **5** and showed only small random fluctuations for **10**. The data were processed,[106] corrected for Lorentz and polarization effects, decay (for **5**), and absorption (empirical, based on azimuthal scans).

The structures were solved by the Patterson method. The asymmetric unit of **10** contains half of a toluene molecule. The toluene is disordered about an inversion center and was modeled by two full-occupancy (overlapping) carbon atoms and three half-occupancy carbon atoms. All non-hydrogen atoms were refined with anisotropic thermal parameters. Hydrogen atoms were fixed in idealized positions (staggered methyl groups, C−H = 0.98 Å, $B_H = 1.2\ B_{\text{bonded atom}}$). Secondary extinction corrections (Zachariasen type, isotropic) were applied, the final values of the extinction coefficients being $3.4(2) \times 10^{-7}$ for **5** and $7.5(12) \times 10^{-7}$ for **10**. Neutral atom scattering factors and anomalous dispersion corrections were taken from the *International Tables for X-ray Crystallography*.[107] Selected bond lengths and angles appear in Tables 2 and 3. Final atomic coordinates and equivalent isotropic thermal parameters, complete tables of bond lengths and angles, hydrogen atom parameters, anisotropic thermal parameters, torsion angles, intermolecular contacts, and least-squares planes are included as Supporting Information.

Synthesis of $CoCl[N(SiMe_2CH_2PPh_2)_2]$ (1). To a 15 mL THF suspension of $CoCl_2$ (0.35 g, 2.7 mmol) was added dropwise a 10 mL THF solution of $LiN(SiMe_2CH_2PPh_2)_2$ (1.40 g, 2.6 mmol). The light baby blue suspension formed a dark blue solution over 30 min. After overnight stirring the THF was removed in vacuo, the residue extracted with toluene and filtered through Celite, and the toluene evaporated to near dryness. The resulting oil was layered with hexanes and allowed to stand. Two days later crystals of $CoCl[N(SiMe_2CH_2PPh_2)_2]$ (**1**) were collected and dried. Yield: 1.34 g (82%). Anal. Calcd for $C_{30}H_{36}ClCoNP_2Si_2$: C, 57.83; H, 5.82; N, 2.25. Found: C, 57.74; H, 5.87; N, 2.29. ^{1}H NMR (C_6D_6): δ 15.0 (v br, 8H), −5.4 (br, 4H). UV−vis (C_7H_8): 506 ($\epsilon = 330\ M^{-1}\ cm^{-1}$), 602 ($\epsilon = 700\ M^{-1}\ cm^{-1}$), 786 ($\epsilon = 290\ M^{-1}\ cm^{-1}$) nm. MS: *m/e* 622 ($M^+$). $\mu_{\text{eff}} = 4.2\ \mu_B$.

Synthesis of $CoBr[N(SiMe_2CH_2PPh_2)_2]$ (2). To a 15 mL THF suspension of $CoBr_2$ (0.35 g, 1.60 mmol) was added dropwise a 10 mL THF solution of $LiN(SiMe_2CH_2PPh_2)_2$ (0.86 g, 1.61 mmol). A dark blue-green solution formed over 30 min from the light green suspension. After the solution was stirred overnight the THF was removed in vacuo, the residue was extracted with toluene and filtered through Celite, and the toluene was evaporated to near dryness. Crystals of $CoBr[N(SiMe_2CH_2PPh_2)_2]$ (**2**) slowly formed from minimum toluene overnight and then were washed with hexanes, collected, and dried. Yield: 0.76 g (71%). ^{1}H NMR (C_6D_6): δ 15.2 (v br, 8H), −5.2 (br, 4H). UV−vis (C_7H_8): 518 ($\epsilon = 310\ M^{-1}\ cm^{-1}$), 616 ($\epsilon = 530\ M^{-1}\ cm^{-1}$), 792 ($\epsilon = 270\ M^{-1}\ cm^{-1}$) nm. MS: *m/e* 668 ($M^+$). $\mu_{\text{eff}} = 4.1\ \mu_B$.

Synthesis of $CoMe[N(SiMe_2CH_2PPh_2)_2]$ (4). A 10 mL THF solution of $CoCl[N(SiMe_2CH_2PPh_2)_2]$ (**1**) (0.25 g, 0.4 mmol) was cooled to −78 °C and MeLi (0.3 mL, 1.4 M in ether, 0.4 mmol) was added dropwise until the blue color changed to yellow-orange. This was warmed to room temperature and stirred for 30 min, and the THF was removed in vacuo. The residue was extracted with hexanes and filtered through Celite, and the yellow hexanes solution was allowed to slowly evaporate. Yellow crystals of **4** were deposited overnight. Alternately, a 10 mL toluene solution of **1** was titrated with MeLi until the blue color dissipated to yellow-orange. Removal of the toluene and extraction with hexanes as before yielded $CoMe[N(SiMe_2CH_2PPh_2)_2]$ (**4**). Yield: 0.23 g (95%). Anal. Calcd for $C_{31}H_{39}CoNP_2Si_2$: C, 61.78; H, 6.52; N, 2.32. Found: C, 61.64; H, 6.63; N, 2.40. ^{1}H NMR (C_6D_6): δ 9.8 (v br, 8H, *o*-Ph), 8.4 (s, 4H, *p*-Ph), 6.5 (s, 8H, *m*-Ph), −3.3 (br, 12H, Si*Me*$_2$), −6.3 (v br, 4H, C*H*$_2$). MS: *m/e* 602 (M^+), 587 ($M^+ - Me$). $\mu_{\text{eff}} = 2.2\ \mu_B$.

Synthesis of $Co(CH_2Ph)[N(SiMe_2CH_2PPh_2)_2]$ (5). A 10 mL THF solution of $CoCl[N(SiMe_2CH_2PPh_2)_2]$ (**1**) (0.17 g, 0.27 mmol) was cooled to −78 °C and a 5 mL THF solution of KCH_2Ph (0.035 g, 0.27 mmol) was added dropwise. The blue solution rapidly turned dark orange/brown. The reaction was brought to room temperature and after being stirred overnight the THF was removed in vacuo, the residue extracted with ether and filtered through Celite, and hexanes (1:1) were added. Slow evaporation yielded red prisms of $Co(CH_2Ph)[N(SiMe_2CH_2PPh_2)_2]$ (**5**). Yield: 0.10 g (55%). Anal. Calcd for $C_{37}H_{43}CoNP_2Si_2$: C, 65.47; H, 6.38; N, 2.06. Found: C, 65.15; H, 6.33; N, 2.00. ^{1}H NMR (C_6D_6): δ 12.5 (br, 2H, CH_2*Ph*), 8.1 (br, 8H, *m*-Ph), 7.3 (br, overlap), 7.1 (s, overlap), −1.8 (br, 2H, CH_2*Ph*), −4.0 (br, 12H, Si*Me*$_2$). MS: *m/e* 678 (M^+), 587 ($M^+ - C_7H_7$). $\mu_{\text{eff}} = 2.1\ \mu_B$.

Synthesis of $Co(CH_2SiMe_3)[N(SiMe_2CH_2PPh_2)_2]$ (6). A 10 mL THF solution of $CoCl[N(SiMe_2CH_2PPh_2)_2]$ (**1**) (0.16 g, 0.26 mmol) was cooled to −78 °C and a 5 mL toluene solution of $LiCH_2SiMe_3$ (0.024 g, 0.26 mmol) was added dropwise. The flask was brought to room temperature over 10 min during which the blue/green solution turned orange. After being stirred overnight the THF was removed in vacuo and the residue was extracted with hexanes, filtered through Celite and reduced to minimum hexanes. The solution deposited orange crystals in the freezer overnight. Alternately, a 10 mL toluene solution of **1** was titrated with $LiCH_2SiMe_3$ until the blue color changed to orange. Removal of the toluene and extraction with hexanes as before gave $Co(CH_2SiMe_3)[N(SiMe_2CH_2PPh_2)_2]$ (**6**). Yield: 0.090 g (52%). Anal. Calcd for $C_{37}H_{47}CoNP_2Si_3$: C, 60.51; H, 7.02; N, 2.08. Found: C, 60.30; H, 7.34; N, 2.31. ^{1}H NMR (C_6D_6): δ 8.5 (s, 4H, *p*-Ph), 6.3 (br, 8H, *m*-Ph), −4.0 (v br, 12H, Si*Me*$_2$), −9.5 (v br, 9H, Si*Me*$_3$). MS: *m/e* 674 (M^+), 587 ($M^+ - CH_2SiMe_3$). $\mu_{\text{eff}} = 2.1\ \mu_B$.

Synthesis of $Co(C_5H_5)[N(SiMe_2CH_2PPh_2)_2]$ (7). $CoCl[N(SiMe_2CH_2PPh_2)_2]$ (**1**) (0.10 g, 0.16 mmol) was dissolved in 10 mL of toluene. To this was added NaCp·DME (0.028 g, 0.16 mmol) in 10 mL of toluene dropwise to very quickly yield first an orange and then a red/brown solution upon completion of addition. This was stirred overnight then filtered through Celite and pumped to dryness to give a brown/red solid, which was recrystallized from a toluene/hexanes mixture (1:1) standing for 1 week to give brown crystals of $Co(C_5H_5)[N(SiMe_2CH_2PPh_2)_2]$ (**7**). Yield: 0.085 g (82%). Anal. Calcd for $C_{35}H_{41}CoNP_2Si_2$: C, 64.40; H, 6.33; N, 2.15. Found: C, 64.70; H, 6.42; N, 2.01. ^{1}H NMR (C_6D_6): δ 8.1 (br, 8H, *o*-Ph), 7.6 (br, 8H, *m*-Ph), 7.05 (s, 4H, *p*-Ph), 1.0 (br, 12H, Si*Me*$_2$), −11 (v br, 4H, C*H*$_2$), −25 (v br, 5H, Cp). MS: *m/e* 652 (M^+), 587 ($M^+ - C_5H_5$). $\mu_{\text{eff}} = 1.9\ \mu_B$.

Synthesis of $CoCl_2[N(SiMe_2CH_2PPh_2)_2]$ (8). To a 15 mL toluene solution of $CoCl[N(SiMe_2CH_2PPh_2)_2]$ (**1**) (0.15 g, 0.24 mmol) was added excess (0.5 mL) benzyl chloride neat. No immediate color change occurred but overnight stirring gave a brown/red solution. After being stirred for four more days a bright red solution had formed. The solvent was removed in vacuo and the residue was extracted with minimum toluene and filtered through Celite and hexanes were added carefully (1:1). Overnight, red crystals of $CoCl_2[N(SiMe_2CH_2PPh_2)_2]$ (**8**) formed. Yield: 0.090 g (57%). Anal. Calcd for $C_{30}H_{36}Cl_2CoNP_2Si_2$: C, 54.71; H, 5.51; N, 2.13. Found: C, 54.82; H, 5.60; N, 2.20. ^{1}H NMR (C_6D_6): δ 12.1 (br, 12H, Si*Me*$_2$), 9.9 (s, 4H, *p*-Ph), 7.2 (v br, 8H, *o*-Ph), 0.8 (br, 8H, *m*-Ph), −58.4 (v br, 4H, C*H*$_2$). UV−vis (C_7H_8): 326 ($\epsilon = 2380\ M^{-1}\ cm^{-1}$), 488 ($\epsilon = 1770\ M^{-1}\ cm^{-1}$) nm.

(105) Haynes, J. S.; Oliver, K. W.; Rettig, S. J.; Thompson, R. C.; Trotter, J. *Can. J. Chem.* **1984**, *62*, 891.

(106) *teXsan*: *Crystal Structure Analysis Package*; Molecular Structure Corp.: The Woodlands, TX, 1995.

(107) (a) *International Tables for X-ray Crystallography*; Kynoch Press: Birmingham, U.K. (present distributor Kluwer Academic Publishers: Boston, MA), 1974; Vol. IV, pp 99−102. (b) *International Tables for Crystallography*; Kluwer Academic Publishers: Boston, MA, 1992; Vol. C, pp 200−206.

MS: *m*/*e* 657 (M^+), 622 ($M^+ - Cl$). $\mu_{eff} = 3.6\ \mu_B$. Reaction of **1** in neat benzyl chloride solvent proceeded more rapidly to give the identical product.

Synthesis of CoBrCl[N(SiMe$_2$CH$_2$PPh$_2$)$_2$] (9). Method 1. To a 10 mL toluene solution of CoCl[N(SiMe$_2$CH$_2$PPh$_2$)$_2$] (**1**) (0.085 g, 0.14 mmol) was added excess (0.3 mL) neat benzyl bromide. Within 5 min the solution turned from blue to become dark red. After being stirred overnight the solvent was removed in vacuo and the residue was extracted with minimum toluene and filtered through Celite. Hexanes were added carefully (4:1 hexanes:toluene) and left to stand. Overnight red crystals of CoBrCl[N(SiMe$_2$CH$_2$PPh$_2$)$_2$] (**9**) formed. To obtain X-ray quality crystals, hexanes were added carefully to a minimum of toluene containing **9**/**10** and allowed to stand, preferentially generating crystals of **10**·0.5C$_7$H$_8$ over 2 days. Yield: 0.075 g (78%). Anal. Calcd for $C_{30}H_{36}BrClCoNP_2Si_2 \cdot C_7H_8$: C, 51.25; H, 5.16; N, 1.99. Found: C, 51.29; H, 5.08; N, 2.08. ^{1}H NMR (C_6D_6): δ 11.1 (br, 12H, Si*Me*$_2$), 10.0 (s, 4H, *p*-Ph), 8.5 (v br, 8H, *o*-Ph), 1.1 (br, 8H, *m*-Ph), −58.2 (v br, 4H, C*H*$_2$). UV−vis: 330 (ϵ = 2900 M^{-1} cm^{-1}), 496 (ϵ = 1900 M^{-1} cm^{-1}) nm. MS: *m*/*e* 668 ($M^+ - Cl$), 622 ($M^+ - Br$). $\mu_{eff} = 3.0\ \mu_B$.

Method 2. To a 10 mL toluene solution of CoBr[N(SiMe$_2$CH$_2$PPh$_2$)$_2$] (**2**) (0.085 g, 0.13 mmol) was added excess (0.3 mL) neat benzyl chloride. Overnight the solution became dark red and after being stirred for 4 days the solvent was removed in vacuo and the residue was extracted with minimum toluene and filtered through Celite. Hexanes were added carefully (4:1 hexanes:toluene) and left to stand. Overnight red crystals of CoBrCl[N(SiMe$_2$CH$_2$PPh$_2$)$_2$] (**9**) formed.

Synthesis of CoBr$_2$[N(SiMe$_2$CH$_2$PPh$_2$)$_2$] (10). To a 10 mL toluene solution of CoCl[N(SiMe$_2$CH$_2$PPh$_2$)$_2$] (**1**) (0.085 g, 0.14 mmol) or CoBr[N(SiMe$_2$CH$_2$PPh$_2$)$_2$] (**2**) was added excess (0.3 mL) benzyl bromide neat. Within 5 min the solution had become dark red. After being stirred for 4 days (**1**) or overnight (**2**) the solvent was removed in vacuo and the residue was extracted with minimum toluene and filtered through Celite. Hexanes were added carefully (4:1 hexanes: toluene) and left to stand. Overnight red crystals of CoBr$_2$[N(SiMe$_2$CH$_2$PPh$_2$)$_2$]·0.5C$_7$H$_8$ (**10**) formed. Yield: 0.20 g (84%). Anal. Calcd for $C_{30}H_{36}Br_2CoNP_2Si_2 \cdot 0.5C_7H_8$: C, 50.70; H, 5.08; N, 1.77. Found: C, 51.45; H, 5.08; N, 1.77. ^{1}H NMR (C_6D_6): δ 11.1 (br, 12H, Si*Me*$_2$), 10.0 (s, 4H, *p*-Ph), 8.5 (v br, 8H, *o*-Ph), 1.2 (br, 8H, *m*-Ph), −58.0 (v br, 4H, C*H*$_2$). UV−vis: 338 (ϵ = 2900 M^{-1} cm^{-1}), 432 (ϵ = 1370 M^{-1} cm^{-1}), 510 (ϵ = 2070 M^{-1} cm^{-1}) nm. MS: *m*/*e* 747 (M^+), 666 (M^+-Br). $\mu_{eff} = 3.3\ \mu_B$.

Reaction of CoBr[N(SiMe$_2$CH$_2$PPh$_2$)$_2$] (2) with Benzyl Bromide in the Presence of TEMPO. To a 10 mL toluene solution of CoBr[N(SiMe$_2$CH$_2$PPh$_2$)$_2$] (**2**) (0.085 g, 0.14 mmol) was added 10 mg of TEMPO and then excess (0.3 mL) benzyl bromide neat. Within 5 min the solution had become dark red. After overnight stirring the solvent was removed in vacuo and the residue was extracted with minimum toluene, filtered through Celite, and dried again. A ^{1}H NMR spectrum of the residue confirmed the presence of *N*-benzyloxy-2,2,6,6-tetramethylpiperidine (4.82 ppm, OC*H*$_2$Ph); a MS was also obtained (*m*/*e* 247 (M^+)). No bibenzyl was observed.

Reaction of CoMe[N(SiMe$_2$CH$_2$PPh$_2$)$_2$] (4) with MeI: Synthesis of CoI[N(SiMe$_2$CH$_2$PPh$_2$)$_2$] (3). To a 10 mL toluene solution of CoMe[N(SiMe$_2$CH$_2$PPh$_2$)$_2$] (**4**) (0.055 g, 0.090 mmol) was added 1.2 equiv of MeI by quantitative vacuum transfer. Overnight the yellow solution turned light green. After being stirred for one more day the toluene was removed in vacuo to give a green oil which was layered with hexanes to quickly yield green crystals of CoI[N(SiMe$_2$CH$_2$PPh$_2$)$_2$] (**3**). Yield: 0.060 g (95%). Anal. Calcd for $C_{30}H_{36}CoINP_2Si_2$: C, 50.43; H, 5.08; N, 1.96. Found: C, 50.87; H, 5.00; N, 1.75. ^{1}H NMR (C_6D_6): δ 15.5 (br, 8H), −5 (br, 4H). UV−vis: 538 (ϵ = 227 M^{-1} cm^{-1}), 634 (ϵ = 557 M^{-1} cm^{-1}), 806 (ϵ = 288 M^{-1} cm^{-1}) nm. MS: *m*/*e* 714 (M^+), 587 ($M^+ - I$), 510 ($M^+ - I - C_6H_5$). $\mu_{eff} = 4.3\ \mu_B$.

Reaction of CoMe[N(SiMe$_2$CH$_2$PPh$_2$)$_2$] (4) with MeBr. To a 10 mL toluene solution of CoMe[N(SiMe$_2$CH$_2$PPh$_2$)$_2$] (**4**) (0.097 g, 0.16 mmol) was added 1.2 equiv of MeBr by vacuum transfer. Overnight the yellow solution turned light green. After one more day of stirring the toluene was removed in vacuo to give a green oil that was extracted in hexanes to give a yellow/green solution. Yellow and green crystals formed overnight in the freezer. The yellow solid was identified as starting material by MS and the green solid as CoBr[N(SiMe$_2$CH$_2$PPh$_2$)$_2$] (**2**) by UV−vis, MS, and ^{1}H NMR spectral comparisons with known material.

Reaction of CoMe[N(SiMe$_2$CH$_2$PPh$_2$)$_2$] (4) with Benzyl Halides. To a 10 mL toluene solution of CoMe[N(SiMe$_2$CH$_2$PPh$_2$)$_2$] (**4**) (0.13 g, 0.21 mmol) was added excess (0.3 mL) neat benzyl chloride. The solution immediately turned orange and then green over a few minutes. Overnight the green solution turned red-brown and a purple precipitate had formed. In the case of neat benzyl bromide addition, the solution immediately turned dark orange and then red over a few minutes; a purple precipitate also formed overnight.[102] After being stirred for one more day the toluene was removed in vacuo to give a red oil, the major product and a small amount of purple solid. The red oil (72% yield, benzyl chloride; 80% yield, benzyl bromide) was identified as CoX$_2$[N(SiMe$_2$CH$_2$PPh$_2$)$_2$] (X = Cl (**8**); X = Br (**10**)) by UV−vis and ^{1}H NMR spectroscopy.

Reaction of CoX$_2$[N(SiMe$_2$CH$_2$PPh$_2$)$_2$] (8, 10) with Alkylating Agents. For each reaction approximately 0.02 g (0.03 mmol) of CoX$_2$[N(SiMe$_2$CH$_2$PPh$_2$)$_2$] (**8** or **10**) was dissolved in 10 mL of toluene. Three reactions, each with 1 equiv of MeLi, LiCH$_2$SiMe$_3$, and C$_3$H$_5$MgBr, at room temperature, all produced CoX[N(SiMe$_2$CH$_2$PPh$_2$)$_2$] (**1** or **2**), identified by its UV−vis spectrum. Addition of a further equivalent produced a yellow color, consistent with the formation of CoR[N(SiMe$_2$CH$_2$PPh$_2$)$_2$]. The target molecule Co(R)X[N(SiMe$_2$CH$_2$PPh$_2$)$_2$] was not detected. In the case of LiCH$_2$SiMe$_3$, the reaction was carried out in an NMR tube (C_7D_8 and C_6D_6) and the peaks of **1**, SiMe$_4$ and Me$_3$SiCH$_2$CH$_2$SiMe$_3$ were observed at δ 0.0 and 0.1. Alkylations with 1 equiv of MeLi or MeMgBr at low temperature (−78 °C) changed the deep red solution to a yellow-orange product, which could potentially be Co(Me)X[N(SiMe$_2$CH$_2$PPh$_2$)$_2$]. Upon being warmed to room temperature these solutions turned green and CoX[N(SiMe$_2$CH$_2$PPh$_2$)$_2$] was identified. Addition of PEt$_3$, CO, and py at low or room temperature prior to alkylation did not alter the final results.

Kinetics Measurements. Kinetic measurements on alkyl halide addition to cobalt(II) halides were performed by monitoring the growth of an appropriate wavelength absorbance of the product in the UV−vis spectrum; the band around 500 nm was generally used. Typical metal-complex concentrations were approximately 10^{-4} M, yielding ΔOD values of approximately 1.5 absorbance units. Reactions were conducted under pseudo-first-order conditions; the alkyl halide used was present in at least a 10-fold excess. The rate constant k_{obs} was determined from the slope of the ln A vs time plot. The final second-order rate constant k was determined from the slope of the straight line plot of k_{obs} vs alkyl halide concentration; pseudo-first-order rates at at least three different concentrations of RX were measured.

Acknowledgment. Financial support for this research was generously provided by NSERC of Canada in the form of Research Grants to M.D.F. and R.C.T. and a 1967 Postgraduate Scholarship to D.B.L.

Supporting Information Available: Full discussion of the X-ray structure of **3** and its variable-temperature magnetic behavior, details of the X-ray crystal structure analysis of **3**, for **3**, **5**, **10**, and **13** tables of complete crystallographic data, atomic coordinates and equivalent isotropic thermal parameters, anisotropic thermal parameters, complete listings of bond lengths and angles, and for **5** and **10** tables of torsion angles, intermolecular contacts, and least-squares planes (60 pages, print/PDF). See any current masthead page for ordering information and Web access instructions.

JA9721632